

Lead germanium telluride: a mechanically robust infrared high-index layer

Bin Li · Ping Xie · Suying Zhang · Dingquan Liu

Received: 18 October 2010 / Accepted: 24 January 2011 / Published online: 4 February 2011
© Springer Science+Business Media, LLC 2011

Abstract A mechanically robust infrared high-index coating material is essential to the infrared interference coatings. Lead germanium telluride ($Pb_{1-x}Ge_xTe$) is a pseudo-binary alloy of IV–VI narrow gap semiconductors of PbTe and GeTe. In our investigation, the hardness and Young's modulus of thin films of $Pb_{1-x}Ge_xTe$, which were deposited on silicon substrates using electron beam evaporation, were identified by means of nanoindentation measurement. It is demonstrated that layers of $Pb_{1-x}Ge_xTe$ have greater hardness and Young's modulus compared with those of PbTe. These mechanical behaviors of layers can be linked to a ferroelectric phase transition from a cubic paraelectric phase to a rhombohedral, ferroelectric phase. Moreover, the strength loss in the layers of $Pb_{1-x}Ge_xTe$ can be also explained in light of strong localized elastic-strain fields in concentrated solid solutions. In addition, it is observed that layers of $Pb_{1-x}Ge_xTe$ are highly transparent and refractive in the mid- and long-wave infrared spectral range ($\sim 3\text{--}40\ \mu\text{m}$). A conclusion can be drawn that a mechanically robust infrared high-index layer can be obtained using $Pb_{1-x}Ge_xTe$ as starting materials.

Introduction

A great variety of optical filters is needed in the design of remote sensing instruments [1]. An optical interference filter consists commonly of a stack of transparent layers of alternating high and low refractive index. The design of

various optical interference coatings, such as antireflection, high-reflecting dielectric mirrors, band-pass, and edge filters, is established on the basis of appropriate choice of refractive index, layer thickness, and the number of layers. The greater the ratio of the high to the low index the fewer layers is needed; furthermore, the higher both indices are the smaller the deterioration of transmission or reflection characteristics in non-normal incident light. In particular, high-index coating materials are essential to infrared interference filters because they are indispensably stacked up with layers of larger optical thickness. These layers should be transparent over a wide spectral region in infrared; preferably, they should have a refractive index greater than that of germanium, a commonly used high-index material with an index of 4.1.

Lead telluride (PbTe) is one of the lead chalcogenides, which has found much usefulness in the fields of thermoelectricity and infrared detection. Currently, it dominates the material selection for the design of infrared interference filters operating in the mid- to long-wave infrared both at room and reduced temperatures. The combination of its high index (above 5.5 in the spectral range of long-wave infrared at room temperature), and its advantage of a negative temperature coefficient of refractive index ($-2.0 \times 10^{-3}\ \text{K}^{-1}$), together with the position of fundamental absorption edge, make it much superior to other infrared coating materials. In single-crystal PbTe compounds, the microhardness is relatively a constant of $\sim 30\ \text{HV}$ for the various carrier concentrations [2]. To the best knowledge, no data is reported on hardness of PbTe thin films; however, a layer of PbTe is so soft that it can be scratched easily. As a consequence, an infrared interference filters consisting of layers of PbTe is not robust enough to withstand the damage originated from standard fabrication processing, such as “from wafer to chips”, even

B. Li (✉) · P. Xie · S. Zhang · D. Liu
Shanghai Institute of Technical Physics,
Chinese Academy of Sciences, Shanghai 200083, China
e-mail: binli@mail.sitp.ac.cn

if more robust low-index materials, like ZnSe or ZnS, are chosen as an outermost layer.

Lead germanium telluride ($\text{Pb}_{1-x}\text{Ge}_x\text{Te}$) is a pseudobinary alloy of IV–VI narrow gap semiconductor compounds of PbTe and GeTe , which shows a ferroelectric phase transition from a cubic, rocksalt (O_h) paraelectric phase to a rhombohedral, arsenic-like (C_{3v}) ferroelectric phase [3, 4]. In the past decade, optical constants of thin films of $\text{Pb}_{1-x}\text{Ge}_x\text{Te}$ as a function of wavelength and temperature were studied in more details, both theoretical and experimental [5]. Furthermore, a low-temperature stable infrared narrow-band filter was made using layers of $\text{Pb}_{1-x}\text{Ge}_x\text{Te}$ [6, 7]. However, the investigation into the mechanical properties of layers of $\text{Pb}_{1-x}\text{Ge}_x\text{Te}$ remains to be done, with the exception of the composition dependence of microhardness for both molten and heat-pressed $\text{Pb}_{1-x}\text{Ge}_x\text{Te}$ ingots [8].

The aim of this article, therefore, is to exhibit the data about room temperature Young's modulus and hardness of layers of $\text{Pb}_{1-x}\text{Ge}_x\text{Te}$ deposited on silicon wafers; furthermore, to explore the correlation between composition in layers and their mechanical properties, finally, to combine these results with the investigation into the spectral transmittances and indices of refraction of layers of $\text{Pb}_{1-x}\text{Ge}_x\text{Te}$.

Experimental details

The bulk ingots of $\text{Pb}_{1-x}\text{Ge}_x\text{Te}$ with three Ge concentration x , 0.10, 0.17, and 0.22, together with PbTe , were synthesized at 1100 °C. The inside surfaces of ampoules were pyrolyzed with carbon to avoid reaction of lead with silica. Subsequently, the resulting ingots were held at 700 °C for 24 h, then cooled down to room temperature with a rate of 10 °C/h. Finally, the ingots were crushed into small pieces with an approximate size of 5 mm and used as resources for evaporation.

Deposition of thin films of $\text{Pb}_{1-x}\text{Ge}_x\text{Te}$ was carried out in a KD500 box coater using a type C6 four-pocket electron beam evaporator in a background vacuum 2.0×10^{-3} Pa. A beam current of around 20 mA at a voltage of 6 kV was reached and a graphite line was used. The silicon wafers polished on both sides, with a diameter of 10 mm and a thickness of 0.8 mm, were used as substrates. A flat calotte carrying samples rotated at a rate of 30 rpm to provide good uniformity of thin films. The substrates were heated below by radiation heaters, and temperature was sensed by a platinum resistance temperature transducer pressed against the upper surface of a substrate. The signals from the transducer were transferred out through a set of electric-brush and slip-ring to operate a temperature controller and thus maintained a constant temperature of

150 °C, which is thought as an optimum temperature. Thickness of all layers was monitored by optical reflection and kept in an approximate value of 2 μm. Five samples in each batch were deposited to prove the repeatability.

The crystallographic structures of thin films were studied by X-ray diffraction using $\text{Cu } K_\alpha$ radiation on a D/max 2550V diffractometer from 10° to 68° with an accuracy of 0.02°. The energy-dispersive X-ray analysis (EDX) was done to decide the compositions of thin films from a Horiba EX-220 energy-dispersive X-ray microanalyzer (model 6853-H) attached to the FE-SEM without coating the surfaces of thin films. The optical transmission spectrums were measured using a Perkin Elmer Spectrum GX Fourier-transform infrared spectrometer with a resolution of 4 cm⁻¹ at the normal incidence. The indices of refraction were derivate by fitting measured transmission spectrums using Lorentz oscillator as a dispersion model. More details can be found in the previous studies [5, 9].

Nanoindentation measurements were performed using a Nano Indenter G200 (MTS Cooperation, Nano Instruments, Oak Ridge, TN, USA) with a three-side pyramidal Berkovich diamond indenter of 50 nm radius (faces 65.3° from vertical axis), under the continuous stiffness measurement (CSM) option. In all cases the loading rate was 1 mN s⁻¹. At least ten indents were performed on each layer with a maximum load of 13 mN, accompanied with a corresponding indentation depths no more than 500 nm. Following the analytic method proposed by Oliver and Pharr [10], the average values and standard deviations of the hardness and Young's modulus of thin films were extracted from the load–displacement results. A typical load–displacement curve is presented in Fig. 1 for thin films of $\text{Pb}_{1-x}\text{Ge}_x\text{Te}$ deposited from a resource material with a Ge concentration of 0.17.

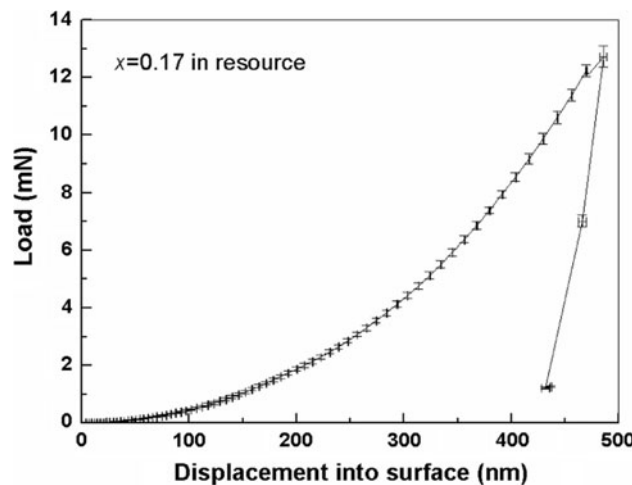


Fig. 1 A typical load–displacement curve for thin films of $\text{Pb}_{1-x}\text{Ge}_x\text{Te}$ deposited from an ingot with a Ge concentration of 0.17, the average values and standard deviations are also shown

Results and discussions

XRD analysis performed on thin films of $\text{Pb}_{1-x}\text{Ge}_x\text{Te}$ reveals all of them are single-phase with polycrystalline characteristics, which suggests the formation of a completed solid solution of PbTe and GeTe. EDX analysis indicates that element of oxygen cannot be found on the surfaces; therefore, the possibility of formation of lead oxide on the surface can be excluded. In addition, other elements related to contaminations are undetectable, either.

In practice, a strictly congruent melt composition will typically not be established due to preferential evaporation losses of one component originated from a large difference between vapor pressures of PbTe and GeTe. Therefore, a more accurate formula $(\text{Pb}_{1-y}\text{Ge}_y)_{1-z}\text{Te}_z$ should be used to designate the corresponding chemical concentration in thin films, in order to distinguish the composition from that in ingot resources. Surprisingly, it can be observed Ge concentration (y) in thin films is in a very good consistence with Ge concentration (x) in ingot resources. A slight excess of tellurium can be also found in thin films, that is, Te concentration (z) has a value greater than 0.5; furthermore, with an increasing of Ge concentration (x) in resources, the excess of tellurium (z) in thin films decreases gradually. A correlation between y and x , accompanied by a variation of z with x , are illustrated in Fig. 2. An eye-guide in the figure labels an exact linear relation of $y = x$.

In Fig. 3, in order to make a comparison, the hardness and modulus of thin films evaporated from ingots with three Ge concentrations x , 0.10, 0.17, and 0.22, together with PbTe, as a function of the displacement of diamond tips which are pressed into the surfaces of thin films, are demonstrated in (a) and (b), respectively. It is obviously shown that thin films of $\text{Pb}_{1-x}\text{Ge}_x\text{Te}$ have a higher value of hardness than that of PbTe. The hardness for sample 3, which was deposited from an ingot with $x = 0.22$, is not high as same as those for sample 1 and 2, which were

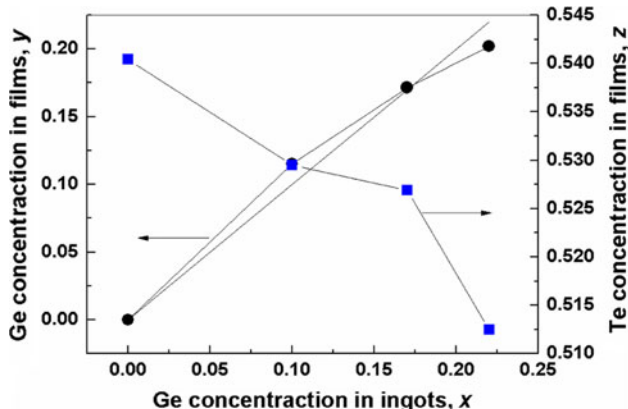


Fig. 2 A comparison of concentrations of Ge and Te in thin films with Ge concentration in ingots

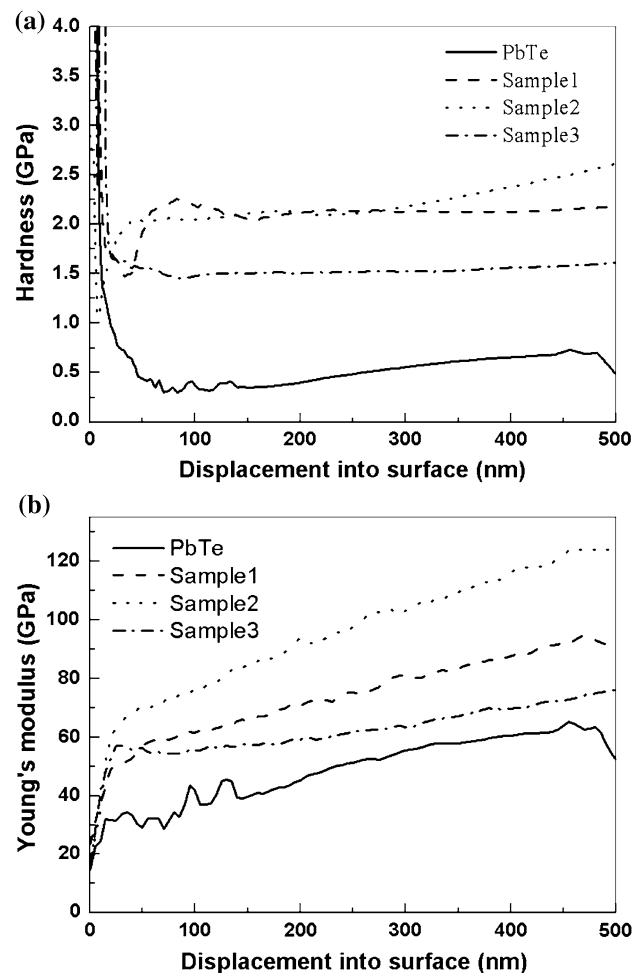


Fig. 3 A comparison of the hardness and Young's modulus of thin films evaporated from ingots with three Ge concentrations x , 0.10, 0.17, and 0.22, to those of PbTe. **a** the hardness. **b** the Young's modulus

deposited from ingots with $x = 0.10$ and 0.17, respectively. A similar tendency can also be found with regard to Young's modulus. As a rule of thumb, to avoid the affect from substrates, a maximum penetration depth (10% of thickness of thin films) is defined as the displacement at which hardness and elastic modulus values are obtained. Therefore, the values of hardness and Young's modulus obtained are listed in Table 1.

Since a complex phase relationships exists for the PbTe–GeTe system, the apparent abnormality in hardness and Young's modulus for sample 3 can be explained in the light of the phase transition from a cubic paraelectric structure to a rhombohedral ferroelectric phase. It was pointed out that, interestingly, although PbTe itself is not ferroelectric, the addition of even 0.05% Ge to PbTe induces the structural transition at Curie temperature T_c , which is a strongly nonlinear function of Ge concentration x , rising from 0 to 230 K from $x = 0.005$ to 0.10 [3, 4]. Moreover, the phase

Table 1 Hardness and Young's modulus obtained at the maximum penetration depth

	Ge concentration x	Hardness (GPa)	Young's Modulus (GPa)
PbTe	0	0.400 ± 0.152	45.379 ± 9.503
Sample1	0.10	2.127 ± 0.187	70.676 ± 3.931
Sample2	0.17	2.119 ± 0.082	94.000 ± 3.700
Sample3	0.22	1.506 ± 0.201	59.249 ± 5.705

transition occurs at room temperature when $x = 0.18$. Therefore, it appears that, at room temperature, a rhombohedral ferroelectric phase structure exists in sample 3; while a cubic paraelectric structure is attributed to sample 1 and 2. To our best knowledge, a similar phenomenon was also observed in random copolymers of vinylidene fluoride (VF_2) and trifluoroethylene (F_3E); and a sharp variation of microhardness can be found at Curie temperature due to a ferro- to paraelectric phase transformation [11]. A conclusion was drawn in the investigation into microhardness in $\text{VF}_2\text{-F}_3\text{E}$ copolymers that the measurement of microhardness is an appropriate technique to accurately detect ferroelectric phase changes. In the PbTe–GeTe system, it should be noted that a change from cubic symmetry to trigonal asymmetry can be remarked by measuring the angular separations of appropriate pairs of reflections, for example, $(\text{hk}0)$ and $(\text{k}0)$, which separates from a single line in the cubic phase, because a gradual variation of the rhombohedral angle emerges from 90° at $x = 0.18$ to almost 88° for $x = 1.0$, i.e., GeTe. However, this evidence can not be provided in the investigations because a greater preferred orientation appears in thin films.

It is usually assumed that the PbTe-based solid solutions, such as $\text{Pb}_{1-x}\text{Ge}_x\text{Te}$, always exhibit a solid solution hardening, that is, a rise in hardness as a function of concentration x . However, in the investigation, it is revealed that sample 1 holds an almost same value in hardness as that for sample 2, although an apparent difference in Ge concentration x exists between 0.10 and 0.17. As a consequence, it can be thought a strength loss occurs in thin films.

It is well known that the mechanical properties of materials depend strongly on the dislocation mobility. However, in the solid solution of PbTe–GeTe, an isovalent substitution of Ge ions for Pb ions results in an insignificant Coulombic interaction between dislocations and substituting ions. As a consequence, electronic subsystem can not create an increase in dislocation mobility, like that usually observed in common semiconductors in low doping levels, such as Ge and Si, accompanied by strength loss [12]. On the one hand, it should be emphasized that a strong localized elastic-strain field is associated with the off-center site occupation of Pb ion sites by Ge ions, due to a

larger difference between their ions radii; on the other hand, the influence of the elastic-strain field on dislocation mobility is very different in concentrated solid solutions from that in a dilute solid solution. The strength loss in thin films of $\text{Pb}_{1-x}\text{Ge}_x\text{Te}$ can probably be explained according to a transition from dilute to concentrated solid solutions. Although the strain fields related to individual Ge substituent in solid solutions can not be simply added up, they have a complex effect on dislocation movement. When the concentration of Ge substituent reaches a critical level, these strong localized elastic-strain fields develop into chains of overlapping strain fields, which can pass through the entire crystalline grain. Therefore, Ge substituents may have a cooperative influence on dislocation movement. In particular, they can notably increase the rate at which double kinks are generated and, hence, increase dislocation velocity and reducing stress [8]. Macroscopically, the strength loss emerges in thin films.

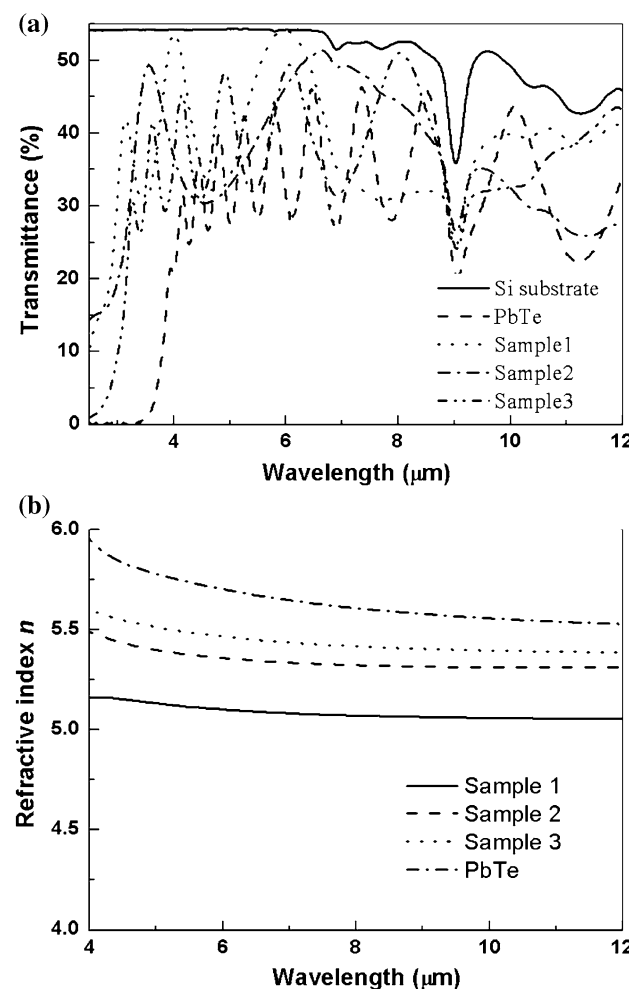


Fig. 4 A comparison of the transmittance and indices of refraction of thin films evaporated from ingots with three Ge concentrations x , 0.10, 0.17, and 0.22, to those of PbTe. **a** the transmittance. **b** the indices of refraction

In Fig. 4a, the transmission spectrums measured for thin films of $\text{Pb}_{1-x}\text{Ge}_x\text{Te}$ evaporated from ingots with three Ge concentrations x , 0.10, 0.17, and 0.22, as well as from PbTe, were presented. It appears that all of thin films are highly transparent. With an increasing of Ge concentration x , the fundamental absorption edge shifts toward long-wavelength. This “red-shift” is quite in a good agreement with that reported in the previous studies [13], which can be attributed to the excess of Te in thin films decreases gradually. The indices of refraction of thin films were demonstrated in Fig. 4b. It can be observed that all of thin films have an index greater than that of germanium; furthermore, the index increases with an increasing of Ge concentration x . A high value can be obtained in sample 3 approaching to that of PbTe.

Conclusion

It can be concluded in the investigation that a mechanically robust layer of $\text{Pb}_{1-x}\text{Ge}_x\text{Te}$ can be evaporated with a high transparency and a high index. However, to take a full of advantage in this wonderful semiconductor, a choice of an appropriate Ge concentration x in the ingots is of importance. A balance must therefore be found between greater hardness and higher index. In the investigation, a Ge concentration $x = 0.17$ seems an optimum condition.

Acknowledgements This study is supported by the National Science Foundation of China (NSFC) under grant no. 60378022 and Excellence Award from President of Chinese Academy of Sciences. Authors would like to thank Prof. X. M. Meng for his helps during EDX analyze and Dr. J. L. Li for his helps in the nanoindentation measurements.

References

1. Hanel RA, Conrath BJ, Jennings DE, Samuelson RE (2003) Exploration of the Solar System by Infrared Remote Sensing, 2nd edn. Cambridge University, New York
2. Crocker AJ, Wilson M (1978) *J Mater Sci* 13:833. doi:[10.1007/BF00570520](https://doi.org/10.1007/BF00570520)
3. Hohnke DK, Holloway H, Kaiser S (1972) *J Phys Chem Solid* 33:2053
4. Dahan SI, Gelbstein Y (2008) *Powder Diffrr* 23:137
5. Li B, Jiang JC, Zhang SY, Zhang FS (2002) *J Appl Phys* 91:3556
6. Li B, Zhang SY, Jiang JC, Fan B, Zhang FS (2004) *Opt Express* 12:401
7. Li B, Zhang SY, Jiang JC, Liu DQ, Zhang FS (2005) *Opt Express* 13:6376
8. Rogacheva EI, Tavrina TV, Krivul'kin IM (1999) *Inorg Mater* 35:236
9. Su WT, Li B, Liu DQ, Zhang FS (2007) *J Phys D* 40:3343
10. Oliver WC, Pharr GM (1992) *J Mater Res* 7:1564
11. Balta Calleja FJ, Santa Cruz C, Gonzalez Arche A, Lopez Cabarcos E (1992) *J Mater Sci* 27:2124. doi:[10.1007/BF01117926](https://doi.org/10.1007/BF01117926)
12. Feltham P, Banerjee R (1992) *J Mater Sci* 27:1626. doi:[10.1007/BF00542926](https://doi.org/10.1007/BF00542926)
13. Li B, Zhang SY, Xie P, Liu DQ (2009) *SPIE Proc* 7282:2L1